Impact of consumer–resource dynamics on C. elegans–E. coli *system exposed to nano zero-valent iron (nZVI)*

Ying-Fei Yang, Chi-Yun Chen, Tien-Hsuan Lu & Chung-Min Liao

Environmental Science and Pollution Research

ISSN 0944-1344
Volume 27
Number 4

Environ Sci Pollut Res (2020)
27:4206-4218
DOI 10.1007/s11356-019-06903-3

Springer

Environmental Science and Pollution Research (2020) 27:4206–4218
https://doi.org/10.1007/s11356-019-06903-3

RESEARCH ARTICLE

Impact of consumer–resource dynamics on *C. elegans–E. coli* system exposed to nano zero-valent iron (nZVI)

Ying-Fei Yang[1] · Chi-Yun Chen[1] · Tien-Hsuan Lu[1] · Chung-Min Liao[1]

Received: 17 April 2019 / Accepted: 28 October 2019 / Published online: 11 December 2019

Abstract

Nano zero-valent iron (nZVI) is one of the most paramount nanoparticles (NPs) applied in environmental remediation, leading to great concerns for the potential impacts on soil ecosystem health. The objective of this study was to link toxicokinetics and consumer–resource dynamics in the *Caenorhabditis elegans–Escherichia coli* (worm–bacteria) ecosystem. The biokinetic parameters of bacteria and worms were obtained from toxicokinetic experiments and related published literature. Biomass dynamics of bacteria and worms were estimated by employing the modified Lotka–Volterra model. Dynamics of bacteria and worm biomass, internal concentrations of nZVI, bioconcentration factors (BCFs), and biomagnification factors (BMFs) were simulated based on the consumer–resource dynamics. Results showed that the biomass of worms steadily increased from 22.25 to 291.49 g L^{-1}, whereas the biomass of bacteria decreased from 17.17 to 4.70×10^{-8} g L^{-1} after 96-h exposures of nZVI. We also observed ratios of nZVI concentrations in worms and bacteria increased from 0.06 to 26.60 after 96 h. Moreover, decrements of the bioconcentration factor of *E. coli* (BCF_E) values from 0.82 to 0.03 after 96 h were observed, whereas values of BMFs increased from 0.06 to 57.62 after 96 h. Internal concentrations of nZVI in worms were found to be mainly influenced by the ingestion rate of bacteria by worms, and the biomass conversion of bacteria had the lowest effect. Implementation of the integrated bioaccumulation–consumer–resource model supports the hypothesis that the *C. elegans–E. coli* dynamics of internal nZVI concentrations could be effectively associated with the predator–prey behavior and was dominated by the same physiological parameter in the two biological systems.

Keywords Nano zero-valent iron · Toxicokinetics · Consumer–resource dynamics · *Caenorhabditis elegans* · *Escherichia coli* · Environmental dynamics

Introduction

Nano zero-valent iron (nZVI) has been widely applied in the field of environmental remediation for contaminated groundwater and soils for its low cost and high efficiency (Fajardo et al. 2012; Gil-Díaz et al. 2014; Gomes et al. 2013; Němeček et al. 2014; Wang and Zhang 1997). However, the long-term impacts of nZVI on environmental and human health have raised comprehensive concerns for the ongoing release of large amounts of nZVI into soil ecosystems (Auffan et al. 2008; Barnes et al. 2010; El-Temsah and Joner 2012; Kadar et al. 2012; Keenan et al. 2009; Keller et al. 2012; Ma et al. 2013; Pawlett et al. 2013; Saccà et al. 2014). Although the potential toxicities of nZVI have been assessed in various ecological indicators and human cell line models (Chen et al. 2013; Keenan et al. 2009; Keller et al. 2012), little is explored in the predictive toxicology field for the nZVI-stressed population dynamics in soil ecosystems based on a mechanistic prospective.

Given the increasing knowledge in nanotoxicology of nZVI, population responses posed by nZVI toxicity such as the predator–prey dynamics should be rigorously estimated to provide a clear understanding of critical toxic effects spanning over different ecological layers of biological organizations (Vinken 2013). The invertebrate *Caenorhabditis elegans* is a bacterivorous and soil-dwelling nematode that is ideal for employing as a model organism in assessing the consumer–resource interactions in soil ecosystems because of its

Responsible Editor: Philipp Gariguess

✉ Chung-Min Liao
cmliao@ntu.edu.tw

[1] Department of Bioenvironmental Systems Engineering, National Taiwan University, Taipei 10617, Taiwan, Republic of China

important role in benthic food webs (Schiemer 1975; Traunspurger et al. 1997). *C. elegans* is also a well-characterized and effective model organism in appraising effects of environmental drivers such as nanotoxicity in physiological and ecological interactions in soil ecosystems (Freeman et al. 2000; Peredney and Williams 2000; Roh et al. 2009).

To elucidate impacts of nZVI accumulations on the predator–prey population dynamics of the *C. elegans*–*Escherichia coli* (worm–bacteria) system, a model linking the biokinetics and the consumer–resource dynamics was developed based on results of nZVI toxicity-based toxicokinetic (TBTK) assessment (Yang et al. 2017). The objectives of this study were threefold: (1) to explore mutual effects between biokinetics and consumer–resource dynamics of nZVI accumulations in *C. elegans* and *E. coli*, (2) to analyze the population dynamics of soil communities posed by nZVI toxicity, and (3) to implicate the utilization of the integrated bioaccumulation–predator–prey model in field application for better environmental management in soil ecosystems.

Materials and methods

Physiochemical characterizations of nZVI

Characterization of nZVI had been performed and described specifically in the previous study (Yang et al. 2016). Briefly, the nZVI was synthesized in the presence of carboxymethylcellulose (CMC) to ensure well-distributed solutions without much agglomerations and aggregations of NPs (He and Zhao 2007). Medaka embryo-rearing medium (ERM) was used as the medium during synthesis. Based on measurements of the dynamic light scattering (DLS) machine, the size distribution of the CMC-coated nZVI was estimated by fitting to a lognormal (LN) function ($r^2 = 0.99$) with a geometric mean (gm) of 10.46 nm and a geometric standard deviation (gsd) of 1.14. The dynamic behaviors of CMC–nZVI in the ERM were also comprehensively characterized in previous studies. The pH values were found to change from 7.5 to 6 after 1000-min exposure. Dissolved oxygen (DO) increased from 0 to 5 after 1000-min exposure. Oxidation reduction potential (ORP) changed from 0.22 to 0.1 V after 1000 min (Chen et al. 2012).

Study data

Study data related to the relationships between nZVI concentrations and time-dependent bioaccumulations in *C. elegans* were obtained from the published study of Yang et al. (2017). Briefly, synchronized L1 larvae of wild-type *C. elegans* were treated with 50, 100, 250, and 500 mg L^{-1} carboxymethylcellulose (CMC)-coated nZVI. The exposure medium was dispersed in the medaka embryo-rearing medium (ERM) supplemented with *E. coli* OP50 (optical density (O.D. = 1.1)) in the dark at 20 °C. To more clearly perceive the interactions among the *C. elegans*–*E. coli*–CMC–nZVI system, morphologies of worms exposed to 50, 100, and 500 CMC–nZVI after 96-h exposure and appearances of adherences of CMC–nZVI to worms or bacteria biomass were observed via microscope (Leica, Wetzlar, Germany) on the nematode-growth media (NGM) plates. For the toxicokinetic assessment, worms were exposed to CMC–nZVI for 5 days in the uptake phase and transferred to clean nematode-growth medium (NGM) agar plates for 2 days in the phase of depuration.

Exposure scenario

In the bioaccumulation–consumer–resource dynamic model, the exposure scenario of the *C. elegans*–*E. coli* system posed by various concentrations of CMC–nZVI was adjusted based on the in situ conditions (Cook 2009). Bacteria were supplemented as food sources to worms every day since typically after 20–24 h exposure, cultivated bacteria move from the stationary phase to the death phase that only several cells remain viable in the bacteria growth curve (Cowan and Bunn 2016). The worms were set to encounter fresh (non-exposed) bacteria at the time points of 23, 47, 71, and 95 h by considering decay of bacteria from 20 to 24, 44 to 48, 68 to 72, and 91 to 95 h, respectively, since exposure. Time points of injections of CMC–nZVI into soil ecosystems were once a day and aligned with the supplemental time of bacteria to ensure enough food sources for worms in simulation durations.

Model description

The original predator–prey models deduced by Lotka (1925) and Volterra (1931) have been modified in numerous ways, among which Holling (1959) has improved the model by applying the notion of a predator functional response.

The basic predator–prey model has the structure shown in Eqs. (1) and (2) (Table 1) where N represents the prey density, P the predator density, $f(N)$ the per capita prey growth rate in the absence of predators, and ε the efficiency of a predator in converting consumed prey into predator offspring. The function $g(N,P)$ is the functional response that is Holling type II prey dependent if $g(N,P) = g(N)$ (Holling 1959). As characterized by functional response of Holling type II, $g(N,P)$ is the rate at which a predator consumes prey, followed by the assumption that the predator is limited by its capacity to process the prey as food (Holling 1959).

Equations (1) and (2) could be extended to describe consumer–resource dynamics of *C. elegans* and *E. coli* OP50 as described in Eqs. (3) and (4) (Table 1) where γ_e is the growth rate of bacteria (h^{-1}), K is the bacteria carrying capacity (g L^{-1}), $B(t)$ is the bacteria biomass as a function of

Table 1 Model equations used in the present study (see text for the symbol meanings)

Equation
Basic predator–prey model
$\frac{dN}{dt} = f(N)N - g(N,P)p$, (1)
$\frac{dP}{dt} = \varepsilon g(N,P)P - \mu P$, (2)
Consumer–resource dynamics of *C. elegans* and *E. coli* OP50
$\frac{dB(t)}{dt} = r_e\left(1-\frac{B(1)}{K}\right)B(t) - g\left(\frac{B(t)}{B(t)+D}\right)W(t)$, (3)
$\frac{dW(t)}{dt} = f_g\left(\frac{B(t)}{B(t)+D}\right)W(t) - \mu_C W(t)$, (4)
CMC–nZVI accumulation model in bacteria and worms[a]
$\frac{dC_E(t)}{dt} = k_{1E}C_W - \left(k_{2E} + k_{1f}\left(\frac{W(t)}{B(t)}\right)\mathrm{BMF_C}\right)C_E(t)$, (5)
$\frac{dC_C(t)}{dt} = \left(k_1 + k_{1f}\left(\frac{B(t)}{B(t)+D}\right)\mathrm{BCF_E}\right)C_W - \left(k_2 + k_{2f} + f_g\left(\frac{B(t)}{B(t)+D}\right)\right)C_C(t)$, (6)
Sensitivity ratio
$\mathrm{SR} = \frac{\Delta C/C_o}{\Delta x/x_o}$. (7)

[a] Adapted from Yang et al. (2017)

time (t) (g L^{-1}), $W(t)$ is the worm biomass as a function of time (t) (g L^{-1}), D is the half saturation for bacteria ingestion (g L^{-1}), f is the biomass conversion rate for bacteria ingested by worms (dimensionless), g is the ingestion rate of bacteria by worms (g g^{-1} h^{-1}), and μ_C is the death rate of worms (h^{-1}). The $(B/(B + D))W$ terms represent the conversion of energy from bacteria to worms that $g(B/(B + D))W$ is taken from the bacteria and $fg(B/(B + D))W$ augments to worms.

To quantitatively analyze the predator–prey dynamics of the *C. elegans–E. coli* ecosystem, we refined the dynamic model to describe CMC–nZVI accumulations in bacteria and worms by adopting the concept of consumer–resource dynamics in Eqs. (3) and (4).

The final accumulation model can be described in Eqs. (5) and (6) (Table 1) where $C_E(t)$ is the time-dependent CMC–nZVI concentration in bacteria tissue (g L^{-1}), t is the time of exposure (h), C_W is the CMC–nZVI concentration in water (μg g^{-1}), k_{1E} is the uptake rate constant from waterborne phase by bacteria (g g^{-1} h^{-1}), k_{2E} is the depuration rate constant for CMC–nZVI in bacteria (h^{-1}), $C_C(t)$ is the time-dependent CMC–nZVI concentration in worms (g L^{-1}), k_1 is the uptake rate constant from the waterborne phase by worms (mL g^{-1} h^{-1}), k_{1f} is the uptake rate constant from bacteria by worms (g g^{-1} h^{-1}), BCF_E is the bioconcentration factor for CMC–nZVI in bacteria (L kg^{-1}), k_2 is the depuration rate constant for CMC–nZVI in worms (h^{-1}), k_{2f} is the depuration rate constant for CMC–nZVI from food in worms (h^{-1}), and BMF_C is the biomagnification factor for CMC–nZVI in worms (dimensionless).

Numerical analysis

Equations (3)–(6) are nonlinear and first-order systems of coupled differential ordinary equations. The numerical integration scheme was employed to solve the dynamic systems Eqs. (3)–(6) based on the Runge–Kutter–Verner 4th-order method provided by Berkeley Madonna 8.0.1 (Berkeley Madonna was developed by Robert Macey and George Oster of the University of California at Berkeley). Equations (3)–(6) have been rigorously solved by numerical analysis based on biokinetic parameters obtained from toxicokinetic assessment (Yang et al. 2017) as well as parameters in related published literature.

Parameterization of the consumer–resource dynamic model

Values of parameters applied in the consumer–resource dynamic model are compiled in Table 2. Physiological parameters such as biomass conversion efficiency for ingested bacteria (f), bacteria growth rate (r_e), worm death rate (μ_C), and ingestion rate of bacteria by worms (g) were adopted from related published literature. The carrying capacity of *E. coli* OP50 (K) was referred to the experimental result of bacteria density in saturated state (O.D. = 2.52) (Milo et al. 2010). The half-saturation biomass for bacteria ingestion (D) was determined based on the meta-analysis of empirical regressions that ratios between half-saturation biomass and carrying capacity were approximately 1/10 (Mulder and Hendriks 2014).

Model simulation

Simulations of predator–prey models were performed by Berkeley Madonna 8.0.1. Phase-space plot for population equilibrium of bacteria and worms was derived by using the language R (Version 3.5.1, The R Foundation

Table 2 Parameter values used in the prey–predator population dynamic model

Parameter	Symbol	Value	Reference
Bacteria biomass as a function of time t	$B(t)$ (g L^{-1})	Varied	–
Worm biomass as a function of time t	$W(t)$ (g L^{-1})	Varied	–
Time-dependent CMC–nZVI concentration in bacteria	$C_E(t)$ (μg g^{-1})	Varied	–
Time-dependent CMC-nZVI concentration in worms	$C_C(t)$ (μg g^{-1})	Varied	–
CMC-nZVI concentrations in water	C_w (μg g^{-1})	100	This study
Initial bacteria biomass	B_i (g L^{-1})	17.17 ± 24.17	This study
Initial worm biomass	W_i (g L^{-1})	22.25 ± 19.33	This study
Growth rate of bacteria	r_e (h^{-1})	0.91	Li et al. (2014)
Ingestion rate of bacteria by worms	g (g g^{-1} h^{-1})	0.0142	Spann et al. (2015)
Biomass conversion rate for bacteria ingested by worms	f (g g^{-1})	10	Margerit et al. (2016)
Death rate of worms	μ_C (h^{-1})	0.0041	Wu et al. (2008)
Bacteria carrying capacity	K (g L^{-1})	2.52	Milo et al. (2010)
Half saturation for bacteria ingestion	D (g L^{-1})	2.52	Mulder and Hendriks (2014)
Uptake rate constant of bacteria	k_{1E} (g g^{-1} h^{-1})	0.829 ± 0.520	Yang et al. (2017)
Elimination rate constant of bacteria	k_{2E} (h^{-1})	0.010 ± 0.018	Yang et al. (2017)
Uptake rate constant for waterborne CMC–nZVI by worms	k_1 (mL g^{-1} h^{-1})	0.046 ± 0.034	Yang et al. (2017)
Elimination rate constant for waterborne CMC–nZVI by worms	k_2 (h^{-1})	0.001 ± 0.015	Yang et al. (2017)
Uptake rate constant for foodborne CMC–nZVI by worms	k_{1f} (g g^{-1} h^{-1})	$0.082 \times 10^{-3} \pm 0.034 \times 10^{-3}$	Yang et al. (2017)
Elimination rate constant for foodborne CMC–nZVI by worms	k_{2f} (h^{-1})	0.016 ± 0.013	Yang et al. (2017)
Bioconcentration factor of bacteria	BCF_E (L kg^{-1})	82.90	Yang et al. (2017)
Biomagnification factor for foodborne CMC-nZVI by worms	BMF_C (–)	6.03×10^{-5}	Yang et al. (2017)

for Statistical Computing). Dynamic responses of biomass, BCF_E, BMF_C, and ratios of internal CMC–nZVI concentrations of worms and bacteria were simulated in exposure scenarios of 50, 100, 500, and 1000 mg L^{-1} CMC–nZVI.

Sensitivity analysis

Sensitivity analysis could determine the effects of different variables and the interactions among them with minimum numbers of runs (Box et al. 1978; Berthouex and Brown 1994). A sensitivity analysis was performed to identify the influences of variables in the algorithm on internal concentrations of CMC–nZVI in worms after 24-h exposure. The sensitivity of each physiological parameter was examined by increasing values of each parameter by 10% to iterate the model simulation and to identify significant changes in the modeled internal concentrations. The sensitivity ratios (SRs) were calculated as Eq. (7) (Table 1), where ΔC is the difference between the resulting and original internal concentrations of CMC–nZVI in worms and Δx is the difference between the resulting and initial values of physiological parameters. The overall bioaccumulation–predator–prey model framework and implementations of this study are illustrated in Fig. 1.

Results

Interactions among the consumer–resource–CMC–nZVI system

Figure 2 shows the morphologies of worms exposed to various concentrations of CMC–nZVI after 96 h and the appearances of the interactions among the *C. elegans*–*E. coli*–CMC–nZVI system on the NGM plates. Results showed that adherences of Fe-oxide precipitations to bacteria or worm biomass could be observed in higher exposure concentrations of 100 and 500 mg L^{-1} CMC–nZVI, indicating the important role of *C. elegans*–*E. coli*–CMC–nZVI interactions in influencing internal concentrations of CMC–nZVI in *C. elegans* (Fig. 2c, d). In addition, 500 mg L^{-1} CMC–nZVI was found to be a lethal concentration to *C. elegans* since residues of worm corpses could be detected on the plate after 96-h exposure, revealing that without constant supplements of bacteria as food sources, the simulation duration of higher than 96 h may

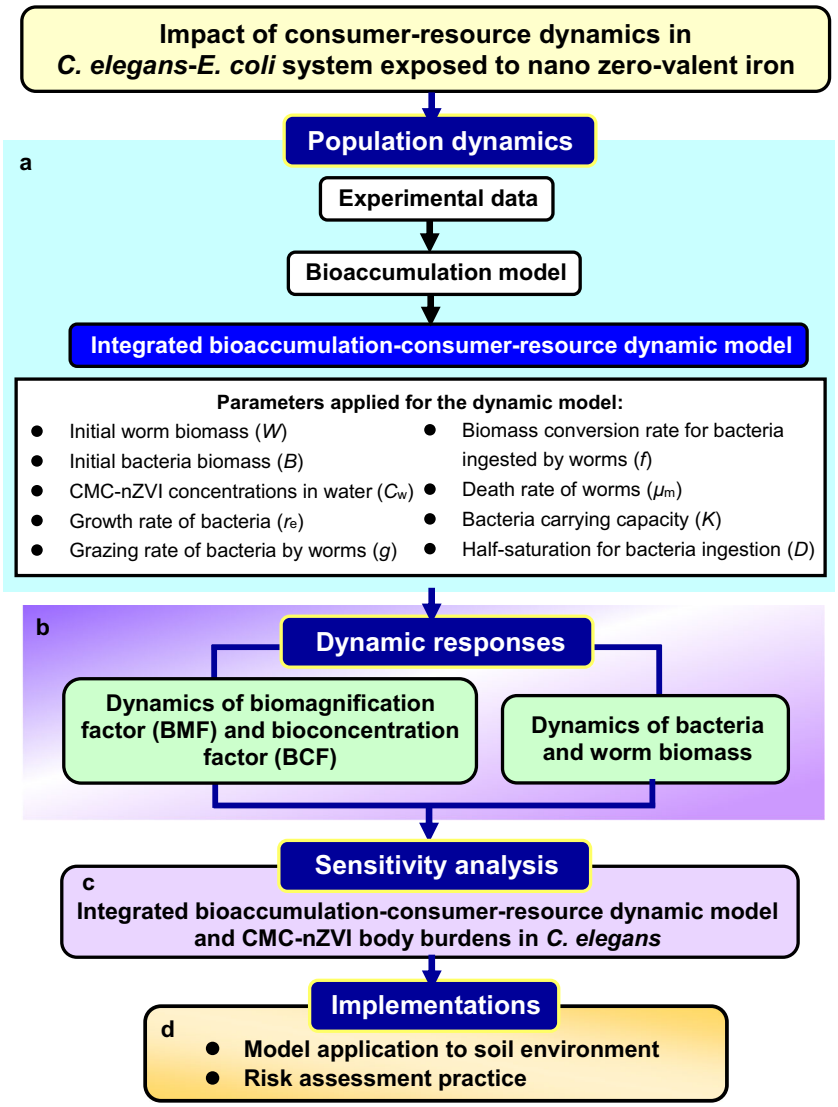

Fig. 1 Schematic showing framework of integrated bioaccumulation–predator–prey model of CMC–nZVI for *C. elegans* in soil ecosystems. (a) Construction of consumer–resource dynamic model based on parameterization from experimental data-derived bioaccumulation model and related published literature, (b) simulated dynamic responses of biomass, BCF, and BMF for *C. elegans* and *E. coli* OP50 and (c) sensitivity analysis of constructed model to CMC–nZVI body burdens in *C. elegans*, and (d) implications in model implementation and risk assessment

not be feasible for worms or bacteria exposed to higher concentrations of CMC–nZVI (Fig. 2d).

Biomass dynamics of *C. elegans* and *E. coli*

The dynamic simulations of bacteria and worm biomass are shown in Fig. 3. Although there was a daily supplement of bacteria in the model simulation, the biomass of bacteria decreased from 17.17 to 4.7×10^{-8} g after 96 h (Fig. 3a). Also, there was a decreased pattern of bacteria biomass before every time point of bacteria supplements that the biomass of bacteria was 1.73, 0.09, and 2.05×10^{-5} g L^{-1} at 23, 47, and 95 h, respectively (Fig. 3a). However, there were continuous increments of worm biomass accompanied with daily supplements of fresh bacteria that worm biomass increased from 22.25 to 291.49 g after 96 h (Fig. 3b). Results also showed that biomass of worms continuously increased after bacteria supplements at 47 and 71 h, and decreased before time points of next supplement due to the continuous decrements of bacteria in the simulation period (Fig. 3).

Population equilibrium of bacteria and worms

As shown in the phase-space plot of bacteria and worms, two equilibrium points were identified when bacteria biomass (B) were 0 and 2.52 g L^{-1} (Fig. 4). However, it could be observed that the population equilibrium of bacteria and worms was achieved when $B = 2.52$ g L^{-1} based on results of trajectories and the ultimate directions of three points with different initial biomass of bacteria and worms (Fig. 4).

Simulations of internal concentrations of CMC–nZVI

Ratios between internal concentrations of CMC–nZVI in bacteria (C_B) and worms (C_C), which is also the definition of the biomagnification factor of *C. elegans*, were simulated in each exposure concentration (Fig. 5). Results showed that ratios

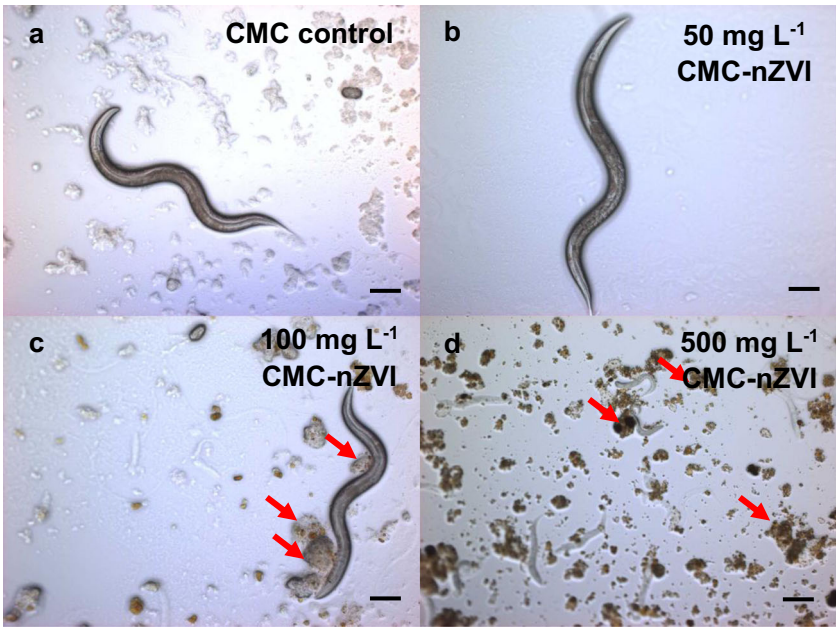

Fig. 2 Representative images of *C. elegans* exposed to **a** CMC control and **b** 50, **c** 100, and **d** 500 mg L^{-1} CMC–nZVI at × 10 magnification. Arrows indicate interactions between bacteria biomass and precipitations of Fe oxides. Scale bars are 100 μm

between C_C and C_B were not influenced by exposure concentrations of CMC–nZVI, and a time-dependent increment of ratios (0.03 to 26.60 from 23 to 95 h) could be observed due to exhaustions of bacteria biomass and decrements of CMC–nZVI concentrations in bacteria during the exposure period (Fig. 5a, b). Consistent with results in Fig. 5a, b, a sudden increase of C_C and C_B ratio from the time point of bacteria supplements from 71 to 95 h was found, revealing the time-dependent dynamics of C_C and C_B ratio due to the decreasing patterns of biomass and internal concentrations of CMC–nZVI in bacteria (Fig. 5c).

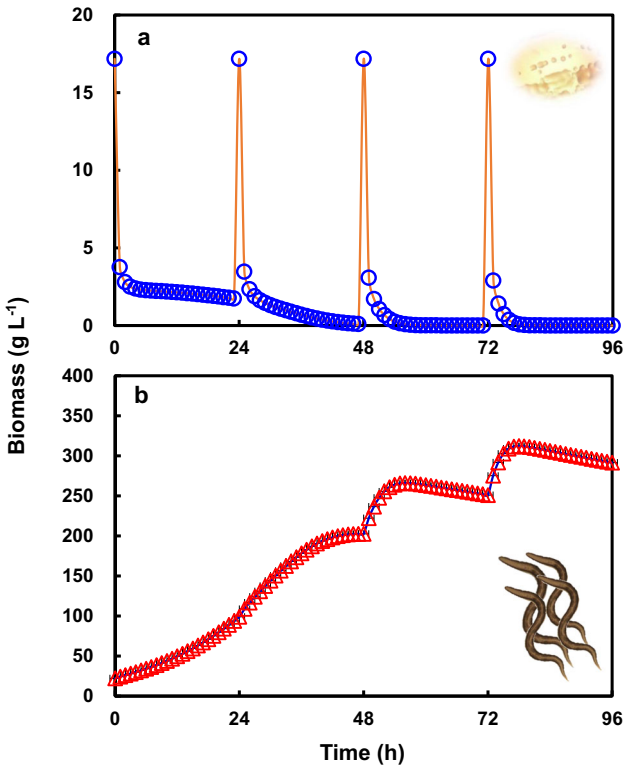

Fig. 3 Simulations for model predictions of (a) bacteria and (b) worms biomass with daily supplements of fresh (non-exposed) bacteria as food sources for 96 h. The initial conditions used were $B(0) = 17.17$ g L^{-1}, $W(0) = 22.25$ g L^{-1}, equilibrium $BCF_E = 82.9$, and equilibrium $BMF_C = 6.03 \times 10^{-5}$. BCF_E = BCF for CMC–nZVI in *E. coli* and BMF_C = BMF for CMC–nZVI in *C. elegans*

Dynamic simulations of BCF_E, and BMF_C

In accordance with the result of dynamic behavior of bacteria biomass, the bioconcentration factor of *E. coli* OP50 (BCF_E) showed a pattern of time-dependent decrement during 96-h exposure, where the BCF_E values decreased from 0.82 to 0.03 from 0 to 96 h (Fig. 6a). Also, values of BCF_E illustrated a decrease pattern at each time point of bacteria supplements (BCF_E = 17.03, 17.03, 15.31, and 0.06 at 23, 47, 71, and 95 h of exposure, respectively) (Fig. 6a). Figure 5b also shows dynamic behaviors of the biomagnification factor of *C. elegans* (BMF_C) that the values exhibited an increasing pattern from 0.06 to 56.62 after 96 h exposure. Also, a continuous increasing trend of BMF_C values after every time point of bacteria supplements could be observed, with values of 0.63, 1.05, 1.51, and 57.62 at 25, 49, 73, and 96 h, respectively (Fig. 5b).

Sensitivity analysis

Among all physiological parameters, the half saturation for bacteria ingestion (D) was the only parameter that

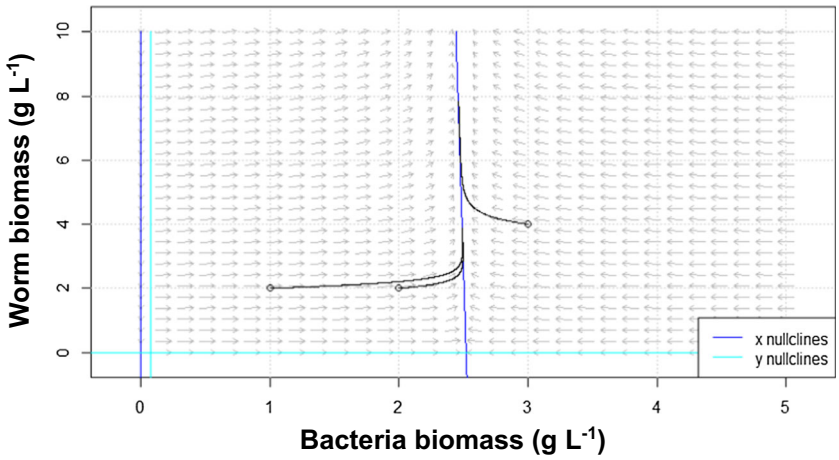

Fig. 4 Phase-space plot for illustrations of population equilibrium at different initial values ((*B*(0) = 1, *W*(0) = 2), (2, 2), and (3, 4))

has a positive value of the sensitivity ratio (SR), indicating its positive influence on internal concentrations of CMC–nZVI in worms (Fig. 7). Results also revealed that the absolute value of the ingestion rate of bacteria by worms (*g*) exhibited the highest SR = 1036.41, followed by death rate of worms (μ_C) (SR = 79.02), carrying capacity (*K*) (SR = 4.73) and growth rate of bacteria (r_e) (SR = 3.96), and biomass conversion rate for bacteria ingested by worms (*f*) (SR = 2.01) for CMC–nZVI concentrations in worms after a 24-h simulation (Fig. 7).

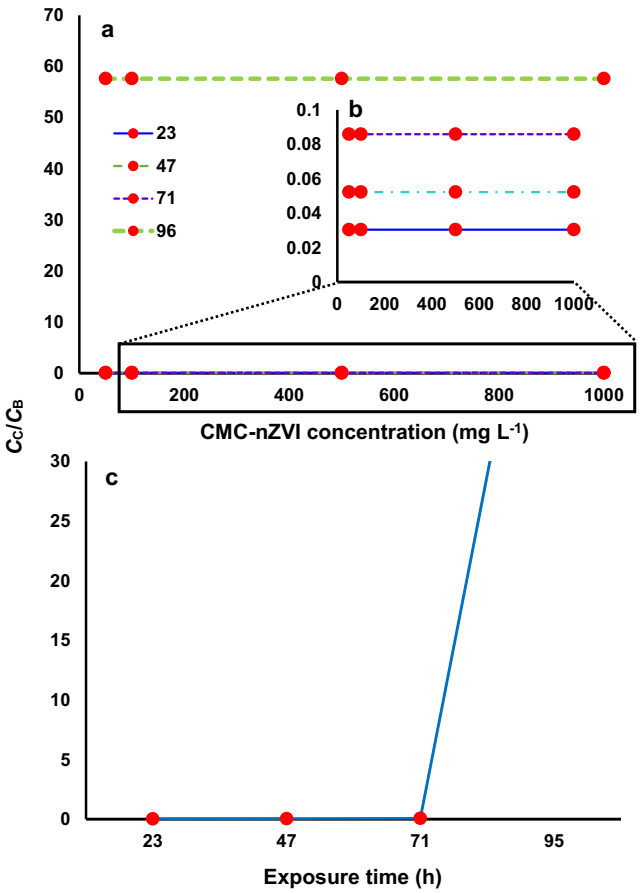

Fig. 5 (A) CMC–nZVI concentration-dependent and (B) time-dependent ratios of internal concentrations of CMC–nZVI in worms (C_C) and bacteria (C_E) at 23, 47, and 71 h as time points of bacteria supplements and 96 h as the simulation period

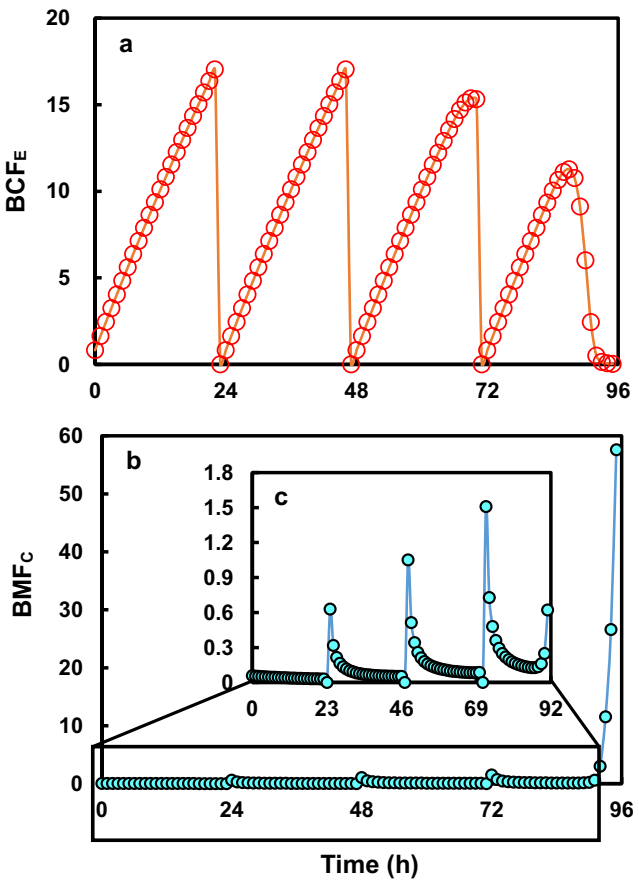

Fig. 6 Simulations for model predictions of (A) BCF_E and (b) BMF_C for 96 h with supplements of fresh bacteria as food sources at 23, 47, and 71 h

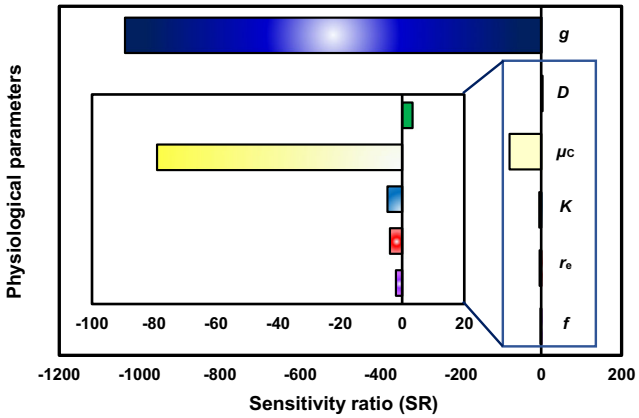

Fig. 7 Sensitivity analysis of each physiological parameter in the integrated bioaccumulation–consumer–resource model

Discussion

Field applications of nZVI

The first field application of nZVI was in 2000. These nanoparticles remained active in the soil for up to 8 weeks (Sarkar et al. 2019). With the tremendous potential in a wide range of environment remediation, the nZVI-based in situ remediation nanotechnology had been conducted or tested at the pilot or field scale at more than 58 nZVI sites, of which 36 were in the USA by 2009 (Karn et al. 2009). In recent years, Bardos et al. (2014) identified around 70 projects documented worldwide at the pilot or full scale. Injection concentrations of nZVI could be ranged from 1000 to 300,000 mg L^{-1} (Gavaskar et al. 2005; Mueller et al. 2012). Past field-scale treatments of pesticide- and high explosives-contaminated soil have used up to 5% (w/w) nZVI (Comfort et al. 2001, 2003).

The nZVI for field applications is typically injected at a soil depth of 3–10 m in suspensions that ranged from 0.2 to 300 g L^{-1} (El-Temsah and Joner 2012; He et al. 2010; O'Carroll et al. 2013). Naja et al. (2008) showed that 6 min was sufficient to degrade 82 mmol L^{-1} RDX (hexahydro-1,3,5-trinitro-1,3,5-triazine) using 300 mg L^{-1} of CMC–nZVI. Zhang et al. (2018) observed that CMC–nZVI could obviously improve the remediation rate of hexavalent chromium-contaminated soil at the dosage of 2.5 g kg^{-1}. Overall, the reported cases and the high injection concentrations indicated the changes of environmental conditions and the potential risks to microbial species and diversity.

Predator–prey dynamics posed by CMC–nZVI toxicity

C. elegans exhibit robust behaviors such as food searching and freely reside in soils, pore water, and sediments (Gray et al. 2005; Hedgecock and Russell 1975). Lee et al. (2017) reported that the foraging behavior of *C. elegans* was modulated by the indole-producing bacteria such as *E. coli*. The predator–prey interaction between *C. elegans* and bacteria was associated with indole-sensing olfactory neurons in *C. elegans*, demonstrating that the bacteriovorous nematode displays vertebrate-like odor receptors to locate bacteria in soils (Choi et al. 2016; Lee et al. 2017). However, since cytotoxicity and bactericidal activities of nZVI have been demonstrated in several studies (Auffan et al. 2008; Barnes et al. 2010; Chaithawiwat et al. 2016; Fajardo et al. 2012; Keenan et al. 2009; Lee et al. 2008; Lefevre et al. 2016), the indole-producing pathway of *E. coli* OP50 could be affected by the exposure of CMC–nZVI, resulting in the bacteria as a less desirable food source for *C. elegans*.

In accordance with experimental results, BMF_C dynamic values were all smaller than 1 (Yang et al. 2017). Bhuvaneshwari et al. (2017) demonstrated that BMF values in the algae–daphnia ecosystem were 0.142 and 0.188 in two kinds of CMC–nZVI coatings. On the other hand, Pawlett et al. (2013) demonstrated that CMC–nZVI toxicity resulted in significant decrements of microbial biomass of gram-negative bacteria. Tilston et al. (2013) also observed that nZVI in high concentration of 10 g kg^{-1} were capable of triggering drastic shift in aquifer indigenous microbial community structure in soils, implicating that the predator–prey dynamic behavior of the *C. elegans–E. coli* OP50 ecosystem will be disrupted if higher concentrations and amounts of CMC–nZVI are applied in soil or groundwater remediation.

Consumer–resource systems display inherent tendency of population cycles (Lotka 1925; Volterra 1926). In the scenario of in situ remediation by CMC–nZVI in groundwater and soils, CMC–nZVI could be injected or pumped into soil ecosystems frequently, resulting in increments of more CMC–nZVI-contaminated soil bacteria. Therefore, although simulated bacteria biomass was degraded to 2.29 g L^{-1} after 24 h, we hypothesize that more bacteria population without CMC–nZVI contamination will encounter freshly injected CMC–nZVI, leading to more CMC–nZVI accumulations in the bacteria population associated with biomass cycling of the *C. elegans–E. coli* predator–prey system.

Farming behavior-associated CMC–nZVI bioaccumulations in *C. elegans*

Thutupalli et al. (2017) demonstrated that the farming behavior of *C. elegans* was attributed to the sticky skin of worms when crawling through a bacterial patch. It was also found that the foraging behavior of *C. elegans* leads to redistribution of bacterial resource, implicating that the CMC–nZVI-bound *E. coli* OP50 could be redistributed, resulting in a higher contact rate and bioaccumulation of CMC–nZVI-contaminated bacteria in *C. elegans* (Thutupalli et al. 2017). Furthermore, since *E. coli* OP50 is a gram-negative bacteria in which the outer membrane is negatively charged, the oxidized forms of CMC–nZVI with a positive charge will be more easily

adhered to cell membranes, leading to more CMC–nZVI-contaminated *E. coli* OP50 redistributions in soil ecosystems (Djurišić et al. 2015).

Moreover, Thutupalli et al. (2017) also suggested that the farming behavior of *C. elegans* is not only limited to the worm–bacteria dynamics but also shares similarities with spreading processes of epidemiology and biological interactions such as disease epidemics, seed dispersal, and engineering of organisms' habitatsSubasinghe et al. (2001) found that fish farming behavior was associated with reservoirs of potential coral disease pathogens and the prevalence of coral disease. Lassuy (1980) demonstrated that both *Eupomacentrus lividus* and *Hemiglyphidodon plagiometopon* weeded out macroalgae from their territories and were fed as generalists upon the remaining species, affecting species diversity and the evenness of the respective algal communities. The dynamics in farming behavior were also observed to influence the dispersal of seeds or the carrying of commensal infectious agents by mobile vectors (Brockmann et al. 2006; Hallatschek and Fisher 2014).

Therefore, due to the evidenced farming behavior of *C. elegans* in bacteria foraging, the predator–prey interactions between worms and bacteria could plausibly facilitate the spread and bioavailability of CMC–nZVI in soils by dispersing new *E. coli* colonies (Thutupalli et al. 2017). Although CMC–nZVI toxicity could potentially affect the indole-producing pathway of *E. coli* OP50, making it undesirable as a food source for *C. elegans*, the foraging behaviors of *C. elegans* and physiochemical interactions between *E. coli* and CMC–nZVI are capable of accumulating more CMC–nZVI-contaminated *E. coli* OP50 in worms via foodborne pathway in soil ecosystems (Djurišić et al. 2015; Thutupalli et al. 2017).

Sensitivity analysis

The conventional bioaccumulation models typically consider chemical uptakes via waterborne or foodborne route based on detailed examination and understanding of chemical uptake and depuration in individual organisms (Campfens and Mackay 1997; Gobas 1993; Thomann et al. 1992). However, these models often assume constant feeding and growth rates in subjected organisms, which could be implausible under varying species abundances (Jackson 1996). The consumer–resource model constructed in this study provides an approach to link biokinetic parameters to physiological parameters such as feeding and growth rates that affect CMC–nZVI accumulations in the nematode–bacteria predator–prey system (Spencer et al. 1997).

Food abundances affect toxicant intake of subjected organisms. Our model found that the most sensitive parameter for CMC–nZVI body burdens in *C. elegans* was in the order of biomass conversion rate (f) and ingestion rate of bacteria by worms (g), and growth rate of bacteria (r_e), indicating that the predator–prey model demonstrated strong relationships between CMC–nZVI accumulations and physiological parameters of worms and bacteria. Furthermore, consistent with results of this study, Boyd et al. (2003) performed a bead-ingestion assay to assess effects of metals on feeding behavior of *C. elegans*, demonstrating that ingestion by worms was significantly reduced by metal toxicities and its sensitivity in sublethal assays. It was also found that stress-induced inhibition of feeding is an important survival mechanism that limits intake of toxicants in *C. elegans* or other invertebrates (Jones and Candido 1999), revealing that ingestion rate plays as an essential role in modulating interactions and accumulations of environmental contaminants in organisms.

Limitations and implications

There have been inevitable time-dependent agglomerations of nZVI in dosing solutions containing worms and bacteria. Sources of agglomerations were mostly from CMC–nZVI and Fe oxides. However, according to results of physiochemical characterization (temporal change of iron speciation) of CMC–nZVI, the proportion of CMC–nZVI and Fe oxides decreased time dependently (decreased from 100 to 20 mg L^{-1} after 1000 min). Therefore, in the bioaccumulation assay, although NPs and Fe oxides adhered to worms and bacteria were inevitable and also limitations that could not be fully considered in model construction, proportions of NPs and Fe oxides were ignorable at least after 24 h.

In addition, although there were agglomerated forms of CMC–nZVI during experimentations, the agglomerated particles could be quantified in the colorimetric assay after digestion with HCl. Total iron concentrations (e.g., CMC–nZVI, Fe oxides, soluble Fe(II) and Fe(III)) were quantified as internal concentrations of worms and bacteria in different sampling times. The disadvantage of this assay was that the agglomerated NPs or Fe oxides adhered on worms and bacteria were measured as internal concentrations during experimentations, which could cause uncertainties in model simulations. Therefore, since the integrated bioaccumulation–consumer–resource model was simulated by adopting parameters from the original toxicokinetic model, the agglomeration phenomenon mentioned above may cause uncertainties in model simulations. More accurate simulation results could be derived from well-designed experimentations that could differentiate CMC–nZVI in internal and surface of worms and bacteria.

Another limitation is that the consumer–resource model could only reflect time-dependent biomass of worms and bacteria posed by exposures of different nZVI concentrations in the worm–bacteria system. The model could be enhanced by enabling variables of $B(t)$ and $W(t)$ to be functions of time and

CMC–nZVI concentrations by applying more experimental results of dynamic change of biomass in more dosing solutions.

Biological systems are continuously exposed to natural or anthropogenic nanomaterials. However, limited literature has explored nanomaterial–biological interactions in the complex biosystems (Hochella Jr et al. 2019). Accelerations of urbanizations will also influence nanomaterial-mediated processes, leading to localized impacts on environmental and human health in the built environment (Baalousha et al. 2016; Hochella Jr et al. 2019). Continuous developments in approach such as analytical techniques, computational simulations, and conceptual models could give insights into the holistic sense of nanomaterial–biological interactions (Hochella Jr et al. 2019). Given that the conventional bioaccumulation model and the population dynamic models are affected by the same factors (Ferson 1996), the integrated bioaccumulation–predator–prey model could provide automatic cross-check on initial assumptions in measured biomass and estimated biokinetic parameters as well as insights into the predator–prey interactions of *C. elegans* and *E. coli* OP50.

Apart from the predator–prey relationship between *C. elegans* and *E. coli* OP50, the biotic environment of *C. elegans* also includes interactions with competitors, parasites (e.g., microsporidia, the Orsay virus, or the fungus *D. coniospora*), predators (e.g., motes, collembola, and nematode-trapping fungi), vectors (e.g., slugs, snails, or isopods), pathogens, and associated microorganisms such as commensals and mutualists (Schulenburg and Félix 2017), implicating that the foraging behaviors of *C. elegans* could result in higher CMC–nZVI bioaccumulations in other soil organisms interacting with the nematodes.

Moreover, it should be noted that the functional response of Holling type II theory proposed that the intake rate of a consumer is the function of resource/prey density (Holling 1959). Also, Hohberg and Traunspurger (2005) reported that the predation rate was positively correlated with prey density that is dependent on the highest biomass uptake per time, revealing that the ingestion rate (g) could be varied with biomass dynamics of bacteria, leading to various CMC–nZVI bioaccumulations in *C. elegans*. To solve this predicament in analyzing the accurate ingestion rate by consumers, Rodríguez-Palero et al. (2018) developed an approach allowing kinetic measurements of food intake by worms at specific time points and alternations of the ingestion rate when subjected to external environmental drivers, suggesting that results derived from the present bioaccumulation–predator–prey dynamic framework could be solidly improved by incorporating rigorous experimental methodologies to obtain more accurate physiological parameters.

In our model setting of the *C. elegans–E. coli* system, the model has the potential to be applied in exploring the adverse effects of CMC–nZVI on consumer–resource interactions of worms and bacteria in the soil ecosystem. Since the nematode has been a large population in various trophic levels of the soil ecosystem, *C. elegans* could be chosen as a bio-indicator to reflect soil health. Application of the integrated bioaccumulation–consumer–resource model can give insights into the ecotoxicity of nZVI (or other kinds of NPs) in the soil ecosystem, by evaluating biomass dynamics and nZVI bioaccumulations in organisms through consumer–resource interactions.

In addition, the constructed model could be extensively employed to assess potential adverse effects of xenobiotics on different ecosystems (e.g., aquatic or terrestrial). In the context of the increasing release of NPs into the soil ecosystem, the consumer–resource interaction could play a contributing role in the disruptions of soil health. Take nZVI in the soil ecosystem for example; the consumer–resource interaction of worms and bacteria (e.g., farming behavior of *C. elegans*) could contribute to higher prevalence of nZVI, leading to higher exposure frequencies for organisms in other trophic levels. Although the interaction between worms and bacteria could be trivial compared to the whole soil ecosystem, alternations of consumer–resource dynamics in lower trophic levels could provide mechanistic tools for risk assessment to prevent potential risks in the population level. We have added more descriptions regarding practical applications of the model in the manuscript.

Taken together, although there are plausible uncertainties in both the model simulations and the experiments, the integrated model linking TK assessment-derived biokinetic parameters with the concept of predator–prey relationship could be extensively employed in risk analysis of soil ecosystems. Moreover, by adopting knowledge regarding field-based CMC–nZVI environmental concentrations with the constructed model, the adverse outcome pathway of CMC–nZVI could make substantial progress to explore potential risks of CMC–nZVI exposure in population levels (Vinken 2013).

Conclusions

Our novel approach mechanistically provides the predator–prey dynamic model integrated with TK analysis based on empirical data- and literature-derived parameters on bioaccumulations of CMC–nZVI in *C. elegans*. The integrated bioaccumulation–consumer–resource model scheme could essentially reinforce our ability to quantitatively understand environmental risks and population dynamics posed by CMC–nZVI exposure and to sustain soil health by setting appropriate criteria for CMC–nZVI environmental remediation in soil ecosystems. We conclude that the proposed integrated dynamic model scheme could be employed as a toolkit in the practice of risk assessment and provide insights into understanding the environmental dynamics and whole

adverse outcomes of specific environmental pollutants or xenobiotics in various ecosystems.

Funding information This study was supported by a grant from the Ministry of Science and Technology of Taiwan (MOST 105-2313-B002-020-MY3).

Compliance with ethical standards

Conflict of interest The authors declare that they have no competing interests.

Research involving human participants and animal rights The article does not contain any studies with human participants or animals performed by any of the authors.

References

Auffan M, Achouak W, Rose J, Roncato MA, Chanéac C, Waite DT, Masion A, Woicik JC, Wiesner MR, Bottero JY (2008) Relation between the redox state of iron-based nanoparticles and their cytotoxicity toward *Escherichia coli*. Environ Sci Technol 42(17):6730–6735

Baalousha M, Yang Y, Vance ME, Colman BP, McNeal S, Xu J, Blaszczak J, Steele M, Bernhardt E, Hochella MF Jr (2016) Outdoor urban nanomaterials: the emergence of a new, integrated, and critical field of study. Sci Total Environ 557-558:740–753

Bardos P, Bone B, Daly P, Elliott D, Jones S, Lowry G, Merly C (2014) A risk/benefit appraisal for the application of nano-scale zero valent iron (nZVI) for the remediation of contaminated sites. WP9 NanoRem

Barnes RJ, van der Gast CJ, Riba O, Lehtovirta LE, Prosser JI, Dobson PJ, Thompson IP (2010) The impact of zero-valent iron nanoparticles on a river water bacterial community. J Hazard Mater 184(1 – 3):73–80

Berthouex PM, Brown LC (1994) Statistics for environmental engineers, Lewis Publishers. CRC press, Boca Raton

Bhuvaneshwari M, Kumar D, Roy R, Chakraborty S, Parashar A, Mukherjee A, Chandrasekaran N, Mukherjee A (2017) Toxicity, accumulation, and trophic transfer of chemically and biologically synthesized nano zero valent iron in a two species freshwater food chain. Aquat Toxicol 183:63–75

Box GEP, Hunter WG, Hunter JS (1978) Statistics for experimenters: an inttroduction to design, data analysis, and model building. Wiley-Interscience, New York

Boyd WA, Cole RD, Anderson GL, Willians PL (2003) The effects of metals and food availability on the behavior of *Caenorhabditis elegans*. Environ Toxicol Chem 22:3049–3055

Brockmann D, Hufnagel L, Geisel T (2006) The scaling laws of human travel. Nature 439(7075):462–465

Campfens J, Mackay D (1997) Fugacity-based model of PCB bioaccumulation in complex aquatic food webs. Environ Toxicol Chem 31(2):577–583

Chaithawiwat K, Vangnai A, McEvoy JM, Pruess B, Krajangpan S, Khan E (2016) Impact of nanoscale zero valent iron on bacteria is growth phase dependent. Chemosphere 144:352–359

Chen PJ, Tan SW, Wu WL (2012) Stabilization or oxidation of nanoscale zerovalent iron at environmentally relevant exposure changes bioavailability and toxicity in medaka fish. Environ Sci Technol 46(15):8431–8439

Chen PJ, Wu WL, Wu KC (2013) The zerovalent iron nanoparticle causes higher developmental toxicity than its oxidation products in early lifestages of medaka fish. Water Res 47(12):3899–3909

Choi JI, Yoon KH, Subbammal Kalichamy S, Yoon SS, Il Lee J (2016) A natural odor attraction between lactic acid bacteria and the nematode *Caenorhabditis elegans*. ISME J 10(3):558–567

Comfort SD, Shea PJ, Machacek TA, Gaber H, Oh BT (2001) Field-scale remediation of a metolachlor-contaminated spill site using zerovalent iron. J Environ Qual 30(5):1636–1643

Comfort SD, Shea PJ, Machacek TA, Satapanajaru T (2003) Pilot-scale treatment of RDX-contaminated soil with zerovalent iron. J Environ Qual 32(5):1717–1725

Cook SM (2009) Assessing the use and application of zero-valent iron nanoparticle technology for remediation at contaminated sites. Office of Solid Waste and Emergency Response, Office of Superfund Remediation and Technology Innovation

Cowan MK, Bunn J (2016) Microbiology fundamentals: a clinical approach, 2nd edn. Hill, McGraw

Djurišić AB, Leung YH, Ng AM, Xu XY, Lee PK, Degger N, Wu RS (2015) Toxicity of metal oxide nanoparticles: mechanisms, characterization, and avoiding experimental artefacts. Small 11(1):26–44

El-Temsah YS, Joner EJ (2012) Ecotoxicological effects on earthworms of fresh and aged nano-sized zero-valent iron (nZVI) in soil. Chemosphere 89(1):76–82

Fajardo C, Ortiz LT, Rodriguez-Membibre ML, Nande M, Lobo MC, Martin M (2012) Assessing the impact of zero-valent iron (ZVi) nanotechnology on soil microbial structure and functionality: a molecular approach. Chemosphere 86(8):802–808

Ferson S (1996) Automated quality assurance checks on model structure in ecological risk assessments. Hum Ecol Risk Assess 2(3):558–569

Freeman MN, Peredney CL, Williams PL (2000) A soil bioassay using the nematode *Caenorhabditis elegans*. In: Henshel DS, Black MC, Harrass MC (eds) Environmental toxicology and risk assessment: standardization of biomarkers for endocrine disruption and environmental assessment. American Society for Testing and Materials, West Conshohocken, pp 305–318

Gavaskar A, Tatar L, Condit W (2005) Cost and performance report: nanoscale zero-valent iron technologies for source remediation. Naval Facilities Engineering Service Center, Port Hueneme

Gil-Díaz MM, Pérez-Sanz A, Vicente MÁ, Lobo MC (2014) Immobilisation of Pb and Zn in soils using stabilised zero-valent iron nanoparticles: effects on soil properties. Clean 42(12):1–9

Gobas FAPC (1993) A model for predicting the bioaccumulation of hydrophobic organic chemicals in aquatic food-webs: application to Lake Ontario. Ecol Model 69(1 − 2):1–17

Gomes HI, Dias-Ferreira C, Ribeiro AB (2013) Overview of in situ and ex situ remediation technologies for PCB-contaminated soils and sediments and obstacles for full-scale application. Sci Total Environ 445–446:237–260

Gray JM, Hill JJ, Bargmann CI (2005) A circuit for navigation in *Caenorhabditis elegans*. Proc Natl Acad Sci U S A 102(9):3184–3191

Hallatschek O, Fisher DS (2014) The acceleration of evolutionary spread by long-range dispersal. Proc Natl Acad Sci U S A 111(46):E4911–E4919

He F, Zhao D (2007) Manipulating the size and dispersibility of zerovalent iron nanoparticles by use of carboxymethyl cellulose stabilizers. Environ Sci Technol 41(17):6216–6221

He F, Zhao D, Paul C (2010) Field assessment of carboxymethyl cellulose stabilized iron nanoparticles for in situ destruction of chlorinated solvents in source zones. Water Res 44(7):2360–2370

Hedgecock EM, Russell RL (1975) Normal and mutant thermotaxis in the nematode *Caenorhabditis elegans*. Proc Natl Acad Sci U S A 72(10):4061–4065

Hochella MF Jr, Mogk DW, Ranville J, Allen IC, Luther GW, Marr LC, McGrail BP, Murayama M, Qafoku NP, Rosso KM, Sahai N,

Schroeder PA, Vikesland P, Westerhoff P, Yang Y (2019) Natural, incidental, and engineered nanomaterials and their impacts on the Earth system. Science 363(6434)

Hohberg K, Traunspurger W (2005) Predator–prey interaction in soil food web: functional response, size-dependent foraging efficiency, and the influence of soil texture. Biol Fertil Soils 41(6):419–427

Holling CS (1959) The components of predation as revealed by a study of small mammal predation of the European pine sawfly. Can Entomol 91(5):293–320

Jackson LJ (1996) A simulation model of PCB dynamics in the Lake Ontario pelagic food web. Ecol Modell 93(1-3):43–56

Jones D, Candido EPM (1999) Feeding is inhibited by sublethal concentrations of toxicants and by heat stress in the nematode *Caenorhabditis elegans*: relationship to the cellular stress response. J Exp Zool 284(2):147–157

Kadar E, Rooks P, Lakey C, White DA (2012) The effect of engineered iron nanoparticles on growth and metabolic status of marine microalgae cultures. Sci Total Environ 439:8–17

Karn B, Kuiken T, Otto M (2009) Nanotechnology and in situ remediation: a review of the benefits and potential risks. Environ Health Perspect 117(12):1813–1831

Keenan CR, Goth-Goldstein R, Lucas D, Sedlak DL (2009) Oxidative stress induced by zero-valent iron nanoparticles and Fe(II) in human bronchial epithelial cells. Environ Sci Technol 43(12):4555–4560

Keller AA, Garner K, Miller RJ, Lenihan HS (2012) Toxicity of nano-zero valent iron to freshwater and marine organisms. PLoS One 7(8):e43983

Lassuy DR (1980) Effects of "farming" behavior by *Eupomacentrus lividus* and *Hemiglyphidodon plagiometopon* on algal community structure. Bull Mar Sci 30(1):304–312

Lee C, Kim JY, Lee WI, Nelson KL, Yoon J, Sedlak DL (2008) Bactericidal effect of zero-valent iron nanoparticles on *Escherichia coli*. Environ Sci Technol 42(13):4927–4933

Lee JH, Kim YG, Kim M, Kim E, Choi H, Kim Y, Lee J (2017) Indole-associated predator-prey interactions between the nematode *Caenorhabditis elegans* and bacteria. Environ Microbiol 19(5): 1776–1790

Lefevre E, Bossa N, Wiesner MR, Gunsch CK (2016) A review of the environmental implications of in situ remediation by nanoscale zero valent iron (nZVI): behavior, transport and impacts on microbial communities. Sci Total Environ 565:889–901

Li B, Qiu Y, Glidle A, Cooper J, Shi H, Yin H (2014) Single cell growth rate and morphological dynamics revealing an "opportunistic" persistence. Analyst 139(13):3305–3313

Lotka AJ (1925) Elements of physical biology. Williams & Wilkins, Baltimore

Ma X, Gurung A, Deng Y (2013) Phytotoxicity and uptake of nanoscale zero-valent iron (nZVI) by two plant species. Sci Total Environ 443: 844–849

Margerit A, Gomez E, Gilbin R (2016) Dynamic energy-based modeling of uranium and cadmium joint toxicity to *Caenorhabditis elegans*. Chemosphere 146:405–412

Milo R, Jorgensen P, Moran U, Weber G, Springer M (2010) BioNumbers–the database of key numbers in molecular and cell biology. Nucleic Acids Res 38(Database issue):D750–D753

Mueller NC, Braun J, Bruns J, Černík M, Rissing P, Rickerby D, Nowack B (2012) Application of nanoscale zero valent iron (NZVI) for groundwater remediation in Europe. Environ Sci Pollut Res Int 19(2):550–558

Mulder C, Hendriks AJ (2014) Half-saturation constants in functional responses. Glob Ecol Conserv 2:161–169

Naja G, Halasz A, Thiboutot S, Ampleman G, Hawari J (2008) Degradation of hexahydro-1, 3, 5-trinitro-1, 3, 5-triazine (RDX) using zerovalent iron nanoparticles. Environ Sci Technol 42(12): 4364–4370

Němeček J, Lhotský O, Cajthaml T (2014) Nanoscale zero-valent iron application for *in situ* reduction of hexavalent chromium and its effects on indigenous microorganism populations. Sci Total Environ 485–486:739–747

O'Carroll D, Sleep B, Krol M, Boparai H, Kocur C (2013) Nanoscale zero valent iron and bimetallic particles for contaminated site remediation. Adv Water Resour 51:104–122

Pawlett M, Ritz K, Dorey RA, Rocks S, Ramsden J, Harris JA (2013) The impact of zero-valent iron nanoparticles upon soil microbial communities is context dependent. Environ Sci Pollut Res Int 20:1041–1049

Peredney CL, Williams PL (2000) Utility of *Caenorhabditis elegans* for assessing heavy metal contamination in artificial soil. Arch Environ Contam Toxicol 39(1):113–118

Rodríguez-Palero MJ, Lopez-Diaz A, Marsac R, Gemoes JE, Olmedo M, Artal-Sanz M (2018) An automated method for the analysis of food intake behavior in *Caenorhabditis elegans*. Sci Rep 8(1):3633

Roh JY, Sim SJ, Yi J, Park K, Chung KH, Ryu DY, Choi J (2009) Ecotoxicity of silver nanoparticles on the soil nematode *Caenorhabditis elegans* using functional ecotoxicogenomics. Environ Sci Technol 43(10):3933–3940

Saccà ML, Fajardo C, Costa G, Lobo C, Nande M, Martin M (2014) Integrating classical and molecular approaches to evaluate the impact of nanosized zero-valent iron (nZVI) on soil organisms. Chemosphere 104:184–189

Sarkar A, Sengupta S, Sen S (2019) Nanoparticles for soil remediation. In: Gothandam KM, Ranjan S, Dasgupta N, Lichtfouse E (eds) Nanoscience and biotechnology for environmental applications. Springer, Cham, pp 249–262

Schiemer F (1975) Nematoda. In: Curds CR, Hawkes HA (eds) Ecological aspects of used-water treatment. Academic, NY, pp 269–288

Schulenburg H, Félix MA (2017) The natural biotic environment of *Caenorhabditis elegans*. Genetics 206:55–86

Spann N, Goedkoop W, Traunspurger W (2015) Phenanthrene bioaccumulation in the nematode *Caenorhabditis elegans*. Environ Sci Technol 49(3):1842–1850

Spencer M, Ginzburg LR, Goldstein RA (1997) Community-level risk assessment, food chains and bioaccumulation. Environ Prog 19:90–97

Subasinghe RP, Bondad-Reantaso MG, SE MG (2001) Aquaculture development, health and wealth. In: Subasinghe RP, Bueno P, Phillips MJ, Hough C, McGladdery SE, Arthur JR (eds) Aquaculture in the third millenium. Technical Proceedings of the Conference on Aquaculture in the Third Millenium, Bangkok, pp 20–25 February 2000 Available at: http://www.fao.org/DOCREP/003/AB412E/ab412e09.htm

Thomann RV, Connolly JP, Parkerton TF (1992) An equilibrium model of organic chemical accumulation in aquatic food webs with sediment interaction. Environ Toxicol Chem 11(5):615–629

Thutupalli S, Uppaluri S, Constable GW, Levin SA, Stone HA, Tarnita CE, Brangwynne CP (2017) Farming and public goods production in *Caenorhabditis elegans* populations. Proc Natl Acad Sci U S A 114(9):2289–2294

Tilston EL, Collins CD, Mitchell GR, Princivalle J, Shaw LJ (2013) Nanoscale zerovalent iron alters soil bacterial community structure and inhibits chloroaromatic biodegradation potential in Aroclor 1242-contaminated soil. Environ Pollut 173:38–46

Traunspurger W, Bergtold M, Goedkoop W (1997) The effect of nematodes on bacterial activity and abundance in a freshwater sediment. Oecologia 112(1):118–122

Vinken M (2013) The adverse outcome pathway concept: a pragmatic tool in toxicology. Toxicology 312:158–165

Volterra V (1926) Fluctuations in the abundance of a species considered mathematically. Nature 118:558–600

Volterra JL (1931) Variations and fluctuations of a number of individuals in animal species living together. Translation. In: Chapman RN (ed). Animal ecology, McGraw Hill, pp 409–448

Wang CB, Zhang WX (1997) Synthesizing nanoscale iron particles for rapid and complete dechlorination of TCE and PCBs. Environ Sci Technol 31(7):2154–2156

Wu D, Cypser JR, Yashin AI, Johnson TE (2008) The U-shaped response of initial mortality in *Caenorhabditis elegans* to mild heat shock: does it explain recent trends in human mortality? J Gerontol A Biol Sci Med Sci 63(7):660–668

Yang YF, Chen PJ, Liao VH (2016) Nanoscale zerovalent iron (nZVI) at environmentally relevant concentrations induced multigenerational reproductive toxicity in Caenorhabditis elegans. Chemosphere 150: 615–623

Yang YF, Lin YJ, Liao CM (2017) Toxicity-based toxicokinetic/toxicodynamic assessment for bioaccumulation and nanotoxicity of zero-valent iron nanoparticles in *Caenorhabditis elegans*. Int J Nanomedicine 12:4607–4621

Zhang R, Zhang N, Fang Z (2018) In situ remediation of hexavalent chromium contaminated soil by CMC-stabilized nanoscale zero-valent iron composited with biochar. Water Sci Technol 77(6): 1622–1631